Stator Shifting in Dual m-phase SPM Machines With Single-Layer Windings for Space Harmonic Cancellation

I. A. Rudden[1], G. J. Li[1], *Senior Member, IEEE*, Z. Q. Zhu[1], *Fellow, IEEE*, A. Duke[2], Z. Azar[2], and A. Thomas[2]
1, Department of Electronic and Electrical Engineering, The University of Sheffield, Sheffield, UK
2, Siemens Gamesa Renewable Energy Limited, North Campus, Broad Lane, Sheffield, UK
g.li@sheffield.ac.uk.

Abstract—This paper investigates the ability for elimination of unwanted magneto-motive force (MMF) harmonics in fractional slot dual *m*-phase single-layer PM machines. By doubling the number of slots and applying stator shifting, the 1st order and one unwanted higher order winding MMF harmonic can be suppressed. Then, through the addition of a second converter operating at a specified phase shift one higher order harmonic can be eliminated. This work identifies the required shift angle of the second winding set as well as converter phase shift in any dual *m*-phase machine to achieve elimination of an unwanted winding MMF harmonic. This methodology is validated by studying 3- and 5-phase machines through analytical modelling. Then two 3-phase machines, 12-slot/10-pole (12s/10p) and 12s/14p, are investigated using FEA. It is found that the 24s/10p dual 3-phase machine can achieve higher torque than the conventional 3-phase 12s/10p but the 24s/14p dual 3-phase performs worse. However, in both cases the significant suppression of unwanted harmonics reduces the rotor iron losses and PM eddy current loss. As a result, the efficiency of each machine is increased by about 3% over its initial 12-slot counterpart. In particular, the PM eddy current losses are reduced by over 95% leading to a substantial reduction in thermal demagnetization risk. The dual 3-phase single-layer machine is also found to achieve higher torque than two similar topology dual 3-phase double-layer machines while having equivalent PM eddy current losses. Both analytical and numerical results have been validated by a series of tests. A prototype machine has been manufactured to validate EMF, static torque, and efficiency measurements of the proposed machine.

Keywords—Dual 3-phase, concentrated windings, single-layer, stator shifting.

I. INTRODUCTION

Electrical machines are often equipped with either single-layer or double-layer windings. The former has a single coil side in each stator slot whilst the latter has two different coil sides in each stator slot. The main drawback of machines with single-layer windings is the larger number of unwanted harmonics in the armature MMF [1], [2]. This is especially prevalent in machines equipped with fractional slot concentrated windings (FSCW), where the number of slots per pole per phase is less than one, as opposed to traditional integer slot windings [3]. FSCW have been shown to offer numerous advantages over integer slot windings [4] such as shorter end winding length, higher slot fill factor, higher fault tolerance, lower torque ripple, and ease of manufacture [5], [6], [7], [8], [9]. The culmination of these benefits can lead to machines that ultimately offer higher efficiencies and torque performance than integer slot machines. Thus, a machine with single-layer FSCW offers great potential provided the presence of unwanted armature MMF harmonics can be suitably mitigated without moving to double-layer windings.

A common method for harmonic elimination is stator shifting, wherein the number of stator slots is increased, and additional winding sets are placed in the new stator slots [10], [11] [12], [13]. This adds complexity to machine manufacturing, but with a properly selected shift angle one can significantly reduce or even eliminate an unwanted harmonic. Another method is to design a dual 3-phase machine that has two 3-phase sets driven by two independent 3-phase converters [14], [15]. By extending to more phase sets in so called 'multiphase' machines more harmonics can be reduced [16], [17], [18], [19]. Stator shifting has been applied to machines with single-layer windings in literature before [20], [21]. In particular one paper by Feng *et al* compares the performance of two single-layer dual 3-phase machines, one 24-slot/10-pole (24s/10p) and one 24s/14p [22]. However, this work does not demonstrate that the harmonic cancellation of this topology can be extended to *m*-phases, nor does it evaluate the impact that the cancelled harmonic has on machine performance by comparing with 12s/10p and

12s/14p machines. Therefore, this paper serves to outline the potential for harmonic cancellation in any dual *m*-phase machine with single-layer windings as well as the potential improvement to machine performance and efficiency.

This work shows that through combining stator shifting with the use of a second converter, one of the dominant higher order harmonics in *m*-phase machines can be eliminated. This is demonstrated for 3- and 5-phase machines using common slot-pole multiples to show how the design process can eliminate a dominant higher-order harmonic. For the 3-phase example 12s/10p and 12s/14p are used, and for the 5-phase example 20s/18p and 20s/22p are used. All machines have a higher order space harmonic that induces losses primarily in the PMs as well as the rotor core. By doubling the number of slots so the 3-phase machines have 24-slots and 5-phase machines 40-slots, stator shifting can be employed. Together with another converter for the second *m*-phase winding set, the unwanted higher order harmonics can be eliminated. This produces machines that have a significant reduction in rotor core iron losses and PM eddy current loss. After demonstrating the harmonic suppression methodology for *m*-phases, the two 3-phase machines will be compared in terms of electromagnetic torque performance and efficiency. It is found that the proposed methods are more suitable for the 12s/10p machine, wherein the resulting machine yields an increase in achievable average torque, a reduction in torque ripple, and a 3% increase in machine efficiency. However, for the 12s/14p machine, although the method succeeds in reducing the torque ripple, the rotor iron losses and PM eddy current loss such that the machine efficiency is increased by around 3%, the achievable average torque is slightly reduced. The dual 3-phase 24s/10p single-layer machine is compared with two double-layer machines and found to exhibit the highest torque while keeping PM eddy current losses low.

II. WINDING THEORY

A. Stator Shifting with a Second Converter

For an *m*-phase machine with single-layer windings to be feasible it must have a total of 2*m* slots. For this *m*-phase

winding to be balanced against excessive vibrations, each phase should have 2 coils circumferentially opposite resulting in a total number of $4m$ slots. The principle of stator shifting is to double the number of slots and introduce a second m-phase winding set at a specific shift angle (α). This generates a machine with $8m$ slots. The introduction of the shift angle (α) introduces an MMF harmonic that can be out of phase with the harmonic produced by the 1st m-phase winding set thus reducing the unwanted harmonic. If both harmonics have the same amplitude and a phase shift angle of 180 elec. deg., complete elimination can be achieved. The attenuation of selected harmonics, and thus resulting winding factor, can be plotted against this shift angle and has been done so for the 3- and 5-phase harmonics in Fig. 1.

For each hth order harmonic, there are exactly h mechanical shift angles that correspond to perfectly in-phase winding sets and exactly h shift angles that correspond to perfectly anti-phase winding sets. This can be seen in the number of times the winding factor is equal to 0 or 1. When the winding factor is kept as 1, the shift angle is causing constructive superposition of the winding MMF harmonic. When the winding factor is reduced to 0, the shift angle is causing destructive superposition of the winding MMF harmonic. Angles for constructive and destructive harmonic superposition can thus be identified as

$$\theta_{hc} = \frac{2k\pi}{h_c} \tag{1}$$

$$\theta_{hd} = \frac{\pi(2r-1)}{h_d} \tag{2}$$

where θ_{hc} is the shift angle for the winding factor of the working harmonic to remain 1 (constructive superposition), θ_{hd} is the shift angle to achieve harmonic cancellation of the parasitic harmonic (destructive superposition), k is any integer from 1 up to and including the working harmonic h_c, and r is any integer from 1 up to and including the parasitic harmonic h_d. To obtain a shift angle where the working harmonic is kept to a maximum and the parasitic harmonic is minimized as much as possible, the values of θ_{hc} and θ_{hd} must be as close as possible. These required angles have been identified for 3-, 5-, and 7-phase machines and displayed in TABLE I. To ensure a machine with equal tooth widths, the mechanical shift angle α must be a multiple of $2\pi/N_s$, where N_s is the number of slots. For each machine in TABLE I, a shift angle for the second m-phase winding set has been identified that lies between θ_{hc} and θ_{hd} and is also a multiple of $2\pi/N_s$.

The shift angle (α) is always equal to the slot pitch multiplied by the working harmonic, as evidenced in TABLE I. To achieve complete constructive superposition of the working harmonic MMF and total destructive superposition of the parasitic MMF, θ_{hc} and θ_{hd} can be achieved by use of a second converter with a shift angle given by
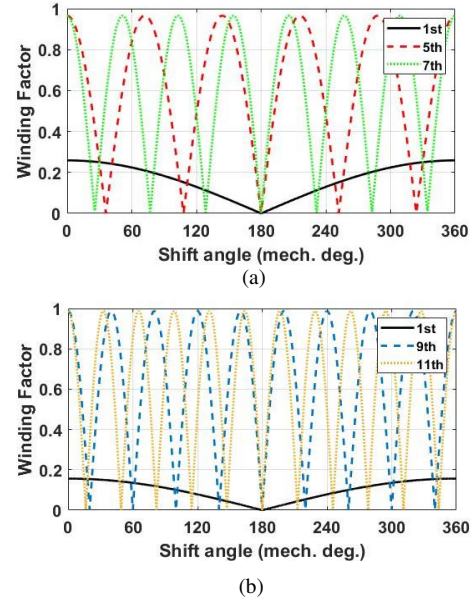

Fig. 1. Winding factor of MMF harmonics *vs* stator shift angle α. (a) 3-phase harmonics, and (b) 5-phase harmonics

$$\theta_c = h_c(\alpha - \theta_{hc}) = h_d(\theta_{hd} - \alpha) \tag{3}$$

An m-phase winding under sinewave current supply is known to produce harmonics of the order

$$h = 2mk \pm 1 \tag{4}$$

where k is any positive integer. Space harmonic waves of the order $h = 2mk + 1$ rotate in the same direction as the fundamental, with space harmonics of the order $h = 2mk - 1$ rotating in the opposite direction. This phenomenon allows for both θ_{hc} and θ_{hd} to be achieved, therefore eliminating the parasitic harmonic while maintaining the working harmonic. Certain columns in TABLE I have been highlighted to show that to design a dual m-phase machine that eliminates a parasitic harmonic completely, only the slot number and pole-pair number are needed. The required shift angle for the second m-phase winding set is the pole-pair number (working harmonic) multiplied by the slot-pitch, and the required phase shift for the second converter is simply equivalent to the slot pitch.

B. Harmonic Cancellation in a 3-Phase Machine

In this section two 3-phase machines, one 12s/10p and one 12s/14p, will be investigated to demonstrate how a chosen parasitic harmonic can be eliminated. For the 12s/10p machine the 5th order harmonic is torque producing with the 1st and 7th order harmonics causing stator and rotor core iron losses and PM eddy current loss. As for the 12s/14p machine the 7th order harmonic is torque producing with the 1st and 5th order harmonics causing losses. Using values taken from Section II.A results in a shift angle (α) of 75 mech. deg. for the 10-pole machine, corresponding to a shift angle of 375 elec. deg. for the 5th order harmonic, and 525 elec. deg. for the

TABLE I SHIFT ANGLES OF CONSTRUCTIVE AND DESTRUCTIVE MMF HARMONICS IN A SELECTION OF M-PHASE MACHINES

m	$N_s/2p$	$2\pi/N_s$	h_c	h_d	θ_{hc}	θ_{hd}	α	$h_c(\alpha-\theta_{hc})$	$h_d(\theta_{hd}-\alpha)$
3	24s/10p	15	5	7	72.0	77.14	75	15	15
	24s/14p	15	7	5	102.86	108	105	15	15
5	40s/18p	9	9	11	80.0	81.8	81	9	9
	40s/22p	9	11	9	98.18	100	99	9	9
7	56s/26p	6.43	13	15	83.08	84	83.56	6.43	6.43
	56s/30p	6.43	15	13	96.0	96.92	96.43	6.43	6.43

7th order harmonic. So, if a second converter is used operating at a 15 elec. deg. phase shift the 5th order harmonic of the two 3-phase sets can be brought perfectly in phase, and since the 7th order harmonic rotates in the opposite direction the harmonics of the two 3-phase sets are brought perfectly anti-phase and so complete cancellation is achieved while keeping the working harmonic (5th) constant. Similarly, in the 14-pole machine 105 mech. deg. corresponds to a shift angle of 735 elec. deg. for the 7th order harmonic and 525 elec. deg. for the 5th order harmonic. Once again using a second converter operating at a phase shift of 15 elec. deg. brings the two 7th order harmonics perfectly in-phase while bringing the two 5th harmonics perfectly anti-phase. The winding layout of a stator shifted machine with two 3-phase winding sets driven by two separate 3-phase converters (24-slot dual 3-phase machine) is shown in Fig. 2. As both 24s/10p and 14p dual 3-phase machines have similar winding layout, only the 24s/10p is shown as an example.

Based on the winding layout shown in Fig. 2, the predicted impact of stator shifting can be calculated using simple calculations of the winding factors of the different harmonics. Winding factor of the hth order harmonic (K_{wh}) is the multiplication of both the coil pitch factor (K_{ph}) and the distribution factor (K_{dh}) and is given by

$$K_{wh} = K_{dh} K_{ph} \qquad (5)$$

The pitch factor can be calculated using the following

$$K_{ph} = \cos(h\gamma/2) \qquad (6)$$

where γ is the difference in span angle (elec. deg.) between the coil and the pole pitches of the hth order harmonic. In this work, the coils of the 24-slot machine span two slots resulting in an equivalent coil pitch to the original 12-slot machine. Thus, the pitch factor for any harmonic will not be impacted by this design. Any harmonic reduction in the 24-slot machine should be determined by the distribution factor given by

$$K_{dn} = sin\left(\frac{rh\sigma}{2}\right) \Big/ \left(r sin\left(\frac{h\sigma}{2}\right)\right) \qquad (7)$$

where r is the number of out of phase coils to be connected in series, and σ is the displacement in space (mech. deg.)

TABLE II DISTRIBUTION FACTORS FOR DIFFERENT HARMONICS OF THE INVESTIGATED 3-PHASE MACHINES

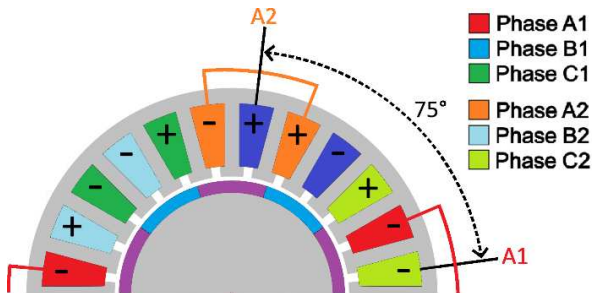|	K_{d1}	K_{d5}	K_{d7}
12s/10p 3-phase	1.0	1.0	1.0
24s/10p 3-phase	0.793	0.991	0.131
24s/10p dual 3-phase	0.701	1.0	0
12s/14p 3-phase	1.0	1.0	1.0
24s/14p 3-phase	0.609	0.131	0.991
24s/14p dual 3-phase	0.701	0	1.0

Fig. 2. Cross-section of half the dual 3-phase 24s/10p machine with single layer windings.

TABLE III DISTRIBUTION FACTORS FOR DIFFERENT HARMONICS OF THE INVESTIGATED 5-PHASE MACHINES

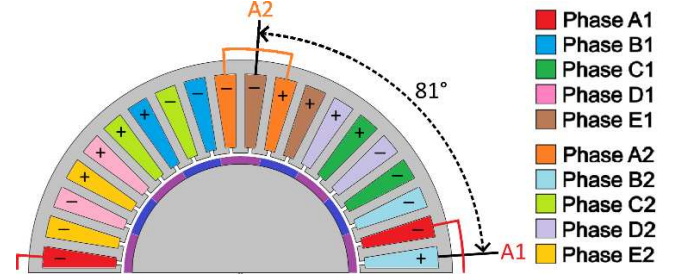|	K_{d1}	K_{d9}	K_{d11}
20s/18p 5-phase	1.0	1.0	1.0
40s/18p 5-phase	0.760	0.997	0.078
40s/18p dual 5-phase	0.705	1.0	0
20s/22p 5-phase	1.0	1.0	1.0
40s/22p 5-phase	0.649	0.078	0.997
40s/22p dual 5-phase	0.705	0	1.0

Fig. 3. Cross-section of half the dual 5-phase 40s/18p machine with single-layer windings

between the series coils. For a conventional 12s/10p or 12s/14p machine with single layer windings all series coils are perfectly in phase and so the distribution factor for all harmonics is 1. For the stator shifted machines such as 24s/10p 3-phase and 24s/14p 3-phase, the mechanical shift angles of 75 mech. deg. and 105 mech. deg. are brought in for the 10-pole and 14-pole variants respectively. This only slightly reduces the distribution factor of the working harmonic while substantially reducing both the 1st order subharmonic and one higher order space harmonic. Finally, the introduction of the second converter to drive the 2nd 3-phase winding set serves to bring the distribution factor of the chosen higher order space harmonic to zero, thus eliminating the harmonic. The full set of distribution factors for the different machines can be seen in TABLE II.

It is unfortunate that in the case of the 24s/14p dual 3-phase machine, the introduction of the second converter increases the distribution factor of the 1st order subharmonic relative to the single 3-phase stator shifted machine (24s/14p 3-phase). However, as complete elimination of the 5th order harmonic is achieved this compromise is acceptable. With the distribution factors calculated we can see that for both the 24s/10p and 24s/14p machines we should expect to see a 29.3% reduction in the 1st order subharmonic in addition to a complete elimination of the chosen higher order harmonic.

C. Harmonic Cancellation in a 5-Phase Machine

Using TABLE I and following the same methodology, the winding schematic for a dual 5-phase 40s/18p machine can be selected and is shown in Fig. 3. The combination of stator shifting in this machine, combined with operating the second converter at a 9° phase shift, will eliminate the unwanted parasitic 11th MMF harmonic. Following the same process as the 3-phase machines, the distribution factors for harmonics in the 5-phase machines can be calculated and are listed in TABLE III. It can be seen that the parasitic harmonic (9th or 11th) is completely removed for the dual 5-phase machines, demonstrating the application of this technique to m-phases.

III. ANALYTICAL MODELLING

A. Calculation of Winding MMF

By way of example, the method is discussed in this section for the 3-phase machines. However, it is very simple to apply the same methodology to multiphase machines and so results for both 3- and 5-phase machines are included. The dimension specifications for these are given in TABLE IV and TABLE V respectively. The armature MMF of a winding can be obtained through the combination of a turn function being fed by a sinewave current. For the first winding set in the 24-slot machine this is given by

$$F_{A1}(\theta, t) = \sum_{k=1,-5,7,\ldots}^{\infty} \frac{6NI_m}{k\pi} \sin\left(\frac{k\pi}{12}\right) \cos(k\theta - \omega t)\cos(\omega t) \quad (8)$$

where N is the number of turns per coil, θ is the angular position in the airgap with reference to the stator, I_m is the peak phase current and ω is the electrical speed. By extending this equation to phases B and C, the armature MMF for a conventional 12-slot machine can be obtained. To calculate the winding MMF for the dual 3-phase 24-slot machines, the above equation is adapted to include the shift angle of the second 3-phase winding set as well as the phase shift of the second converter. The equations for the second phase A in the stator shifted machines can be seen in (9).

$$F_{A2}(\theta, t) = \sum_{k=1,-5,7,\ldots}^{\infty} \frac{6N_c I_m}{k\pi} \sin\left(\frac{k\pi}{12}\right) \cos(k(\theta - \alpha) + \theta_c - \omega t)\cos(\omega t) \quad (9)$$

where θ_c is the phase shift in the second converter (-15 elec. deg. in the 10-pole machine and +15 elec. deg. in the 14-pole), and α is the mechanical shift angle of the second winding set. Once these equations are extended to all three phases, the armature MMF of the 12-slot and 24-slot machines can be obtained, as shown in Fig. 4.

It can be seen in Fig. 4 that both machines successfully suppress the unwanted harmonics (7th order harmonic for the 24s/10p machine and 5th order harmonic for the 24s/14p machine). Additionally, both machines show that the 1st order subharmonic is notably reduced as well. The combination of eliminated higher order harmonics and reduced 1st order subharmonic should reduce the rotor iron losses and PM eddy current loss. Also, the addition of the second converter has allowed the working harmonic to remain constant such that the torque performance should not be impacted by the winding structure. A breakdown of harmonic amplitudes is given in TABLE VI with the values given in p.u. using the corresponding working harmonic as base value. The change in harmonics also corroborates the expected results from the previous calculation of winding harmonic distribution factors in Section II.B, with both machines achieving almost an exact 29.3% reduction in the 1st order subharmonic and a complete elimination of the selected higher order space harmonic.

The same method is then applied for the 5-phase machines and the results are also displayed in Fig. 4 with a breakdown of harmonic amplitudes given in TABLE VII. Successful elimination has been achieved for one parasitic harmonic using this topology in addition to a large reduction of the first

TABLE IV SPECIFICATION OF 3-PHASE INVESTIGATED MACHINES

Slot number	12/24	Stack length (mm)	50
Pole number	10/14	Air-gap length (mm)	1
Rated current (A$_{rms}$)	7.34	Tooth width (mm)	7/3.5
Rated speed (RPM)	400	Tooth height (mm)	2.5
Turns per phase	132/66	Stator yoke height (mm)	3.7
Stator outer radius (mm)	50	Magnet thickness (mm)	3
Rotor outer radius (mm)	27.5	Magnet remanence (T)	1.24

TABLE V SPECIFICATION OF 5-PHASE INVESTIGATED MACHINES

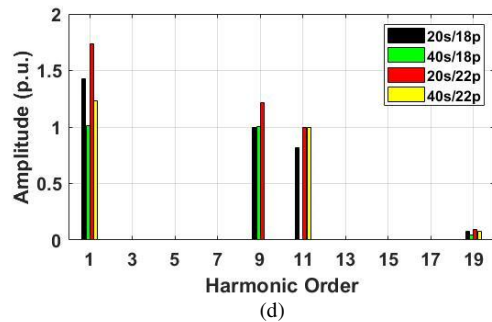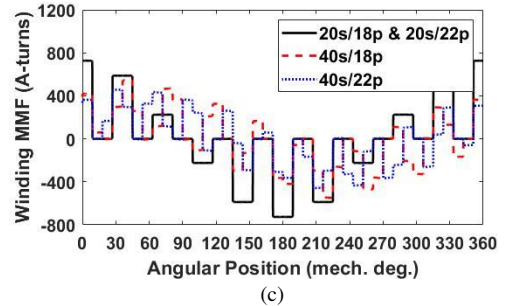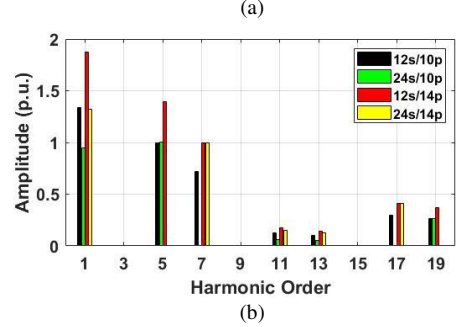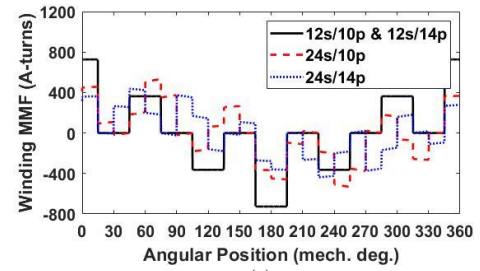| Slot number	20/40	Stack length (mm)	50
Pole number	18/22	Air-gap length (mm)	1
Rated current (A$_{rms}$)	7.34	Tooth width (mm)	5.4/2.7
Rated speed (RPM)	400	Tooth height (mm)	1.9
Turns per phase	132/66	Stator yoke height (mm)	3.9
Stator outer radius (mm)	60	Magnet thickness (mm)	3
Rotor outer radius (mm)	33	Magnet remanence (T)	1.24

Fig. 4. Winding MMF for 3- and 5-phase conventional and dual 3-phase stator shifted machines. (a) 3-phase waveforms, (b) 3-phase spectra, (c) 5-phase waveforms, and (d) 5-phase spectra. Spectra given in p.u. using the corresponding working harmonics as base value.

subspace harmonic. Thus, further demonstrating the application of this method to multiphase machines.

TABLE VI HARMONICS (P.U.) OF ARMATURE MMF IN 10-POLE AND 14-POLE 3-PHASE MACHINES

Harmonic	12s/10p	24s/10p	12s/14p	24s/14p
1st	1.340	0.948	1.872	1.325
5th	1.000	1.001	1.398	0
7th	0.716	0	1.000	0.999

TABLE VII HARMONICS (P.U.) OF ARMATURE MMF IN 18-POLE AND 22-POLE 5-PHASE MACHINES

Harmonic	20s/18p	40s/18p	20s/22p	40s/22p
1st	1.426	1.009	1.738	1.230
9th	1.000	1.001	1.219	0
11th	0.821	0	1.000	0.999

IV. FEA RESULTS

For the purposes of this investigation, the impact of harmonic elimination on machine performance is studied only for the 3-phase machines. This is due to its much wider application in industry than 5- or even larger phase numbered machines. However, as detailed before, should an industry application require a multiphase machine then this winding topology is still an attractive option for minimizing parasitic harmonics.

A. Optimisation Process

OPERA's optimization suite was used to optimize the geometry of the 3-phase machines. The objective of the optimization process was to maximize the average torque of the machine while constraining the current density such that the overall copper area could not be reduced, thus keeping copper losses mostly constant. In addition to this the stator outer radius, rated current, rated speed, air-gap length, magnet volume, number of turns per phase, and stack length were all kept constant. The variables in the optimizations can be seen in TABLE VIII and include: split ratio (s), slot-width to tooth-width ratio (β_s), ratio of slot height to stator core height (h_{sy}), and ratio of tooth tip height to tooth width (t_{hw}). The resulting machine parameters can be seen in TABLE IX with all other parameters remaining the same as given in TABLE IV.

B. Torque Performance

The torques of the optimized machines at rated current have been calculated using FEA models, and the results are shown in Fig. 5. It can be seen for the 10-pole machines that the average torque is very close, as expected based on the equal magnitudes of working MMF harmonic. The 24s/14p machine unfortunately does not achieve an equal torque to the 12s/14p machine. A direct comparison of the torque performances can be seen in TABLE X.

The 24s/10p has achieved an increase of 0.89% in average torque over the original 12s/10p machine while the 24s/14p machine has had its average torque reduced by 3.83%

TABLE VIII OPTIMISATION PARAMETERS

Objective Functions	Maximize Average Torque
Constraints	Maximum Current Density <= 3.336A/mm²
Model Parameters	0.45 <= s <= 0.65 and 0.45 <= β_s <= 0.6
	0.7 <= h_{sy} <= 0.9 and 0.3 <= t_{hw} <= 0.4

TABLE IX OPTIMISED MACHINE DIMENSIONS

	12s/10p	24s/10p	12s/14p	24s/14p
Slot number	12	24	12	24
Tooth width (mm)	6.38	3.60	6.44	3.80
Tooth tip height (mm)	1.93	1.08	1.93	1.14
Rotor outer radius (mm)	29.45	29.0	29.75	30.1
Stator yoke height (mm)	3.44	3.46	3.08	2.48
Magnet thickness (mm)	2.78	2.83	2.75	2.71

TABLE X TORQUE OF 10-POLE AND 14-POLE MACHINES

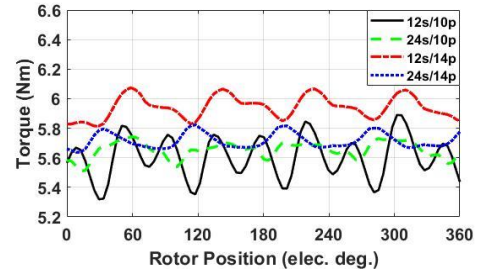|	Average Torque (Nm)	Torque Ripple (Nm)
12s/10p	5.61	0.571 (10.17%)
24s/10p	5.66 (**+0.89%**)	0.233 (4.12%)
12s/14p	5.94	0.259 (4.37%)
24s/14p	5.72 (**-3.83%**)	0.186 (3.25%)

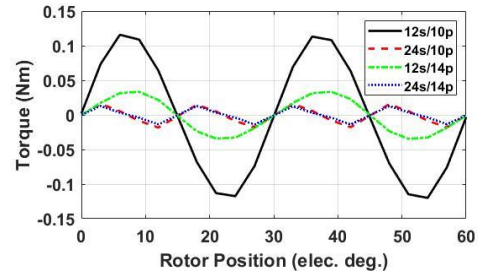Fig. 5. Comparative torque performance of optimized machines.

Fig. 6. Cogging torque comparison of 12-slot and 24-slot machines.
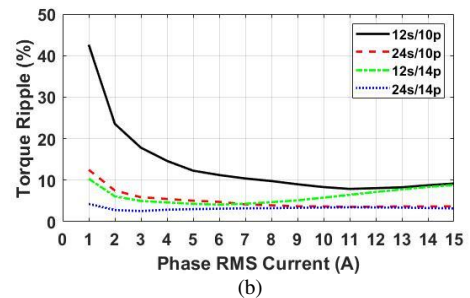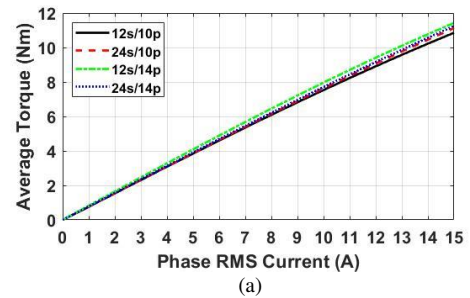

(a)

(b)

Fig. 7. Average torque and torque ripple coefficient versus phase RMS current. (a) Average torque, and (b) torque ripple coefficient.

compared with the original 12s/14p machine. In both cases, the 24-slot machines show a reduction in torque ripple likely due to a reduction in cogging torque, as shown in Fig. 6. As would be expected (see Fig. 6) the cogging torque of the 24-slot machines is less than that of the 12-slot machines due to the lower common multiple between the slot and pole numbers [6]. This undoubtedly helps reduce the torque ripple of the 24-slot machines. To assess the torque performance under a range of operating conditions, the average torque and torque ripple coefficient versus phase RMS current have been calculated, as shown in Fig. 7. There appears to be little split between the 12-slot and 24-slot machine variants at increasing phase currents. The 24s/10p achieves the same average torque

as the 12s/10p machine for low currents and then begins to achieve higher torques once the phase RMS current approaches operating condition. The 24s/14p machine continues to achieve less torque than the 12s/14p machine for all phase RMS currents. Again, the torque ripple of the 24-slot machines is less than their 12-slot counterparts.

C. Losses and Efficiency

Operating the machines at rated speed and rated current also allowed the main losses of the machines under such conditions to be calculated. The flux densities of different harmonics in each mesh element across the stator was calculated. This was then used for calculations of stator hysteresis and eddy current loss. A solid iron rotor was used, so the current density in each mesh element was obtained to calculate the eddy current loss in the rotor core and PMs. For copper loss the following equation was used

$$P_{copper} = N_s N_c^2 \rho \frac{L_w}{S k_b} I_{rms}^2 \qquad (10)$$

where N_s is the number of slots, N_c is the number of conductors per slot, ρ (Ωm) is the resistivity of copper at room temperature, L_w (m) is the sum of both active length and end winding length, S (m^2) is the slot area, k_b is the slot packing factor, and I_{rms} (A) the phase RMS current. The end winding length has been calculated by using the arc-length between the center of two slots. Although the coil pitch of the 24-slot machines is 2, the arc-length between the two slots is the same as in the 12-slot machines. So, this approximation of end winding length gives the same result for the 12-slot and 24-slot machines. This equation only accounts for DC copper losses and so offers a simple approximation for comparing copper losses between machines. Although (10) does not account for any AC winding loss effects, it is deemed appropriate for this investigation as rated speed is relatively low, so the electrical frequency is as well. The power of the machines was calculated from the achieved average torque and rotation speed, and then after incorporating the losses the efficiencies could be calculated. All this is given in TABLE XI for the 10-pole and 14-pole machines. As was expected, the move to 24-slots increases the stator saturation such that the losses in the stator are increased for both the 10-pole and 14-pole machines. This can be seen by comparing the flux density distribution within the 12s/10p and 24s/10p stator teeth, as shown in Fig. 8. The move the 24-slots has increased the peak flux density within the stator teeth from 1.6T to 1.8T, leading to a substantial increase in stator loss. However, the elimination of the unwanted higher order harmonic and reduction of the 1st order subharmonic shows substantial reduction in rotor iron losses and PM eddy current losses. Again, this is because these harmonics rotate asynchronously with the rotor and so they are a primary cause of rotor losses.

TABLE XI LOSSES (IN W) AT RATED OPERATING CONDITIONS FOR 10-POLE AND 14-POLE MACHINES

	Stator Loss	Rotor Loss	PM Loss	Copper Loss	Efficiency (%)
12s/10p	3.80	8.57	1.522	44.60	75.11
24s/10p	4.558	4.728	0.0329	44.33	77.37
	(+19.95%)	(-44.83%)	(-97.84%)		(+3.02%)
12s/14p	3.88	11.42	1.724	44.18	75.40
24s/14p	4.823	4.092	0.0214	44.66	77.63
	(+24.30%)	(-64.17%)	(-98.76%)		(+2.95%)

Note: the percentages given in this table show the variations of losses and efficiency from 12-slot to 24-slot.

The combined reduction in the rotor iron losses and PM eddy current loss has yielded a 3.02% improvement in efficiency of the 24s/10p machine over the 12s/10p machine, and a 2.95% improvement in efficiency of the 24s/14p machine over the 12s/14p machine. A plot of eddy current density in the PMs shows just how much the harmonic elimination successfully reduces the PM eddy current losses, as can be seen in Fig. 9.
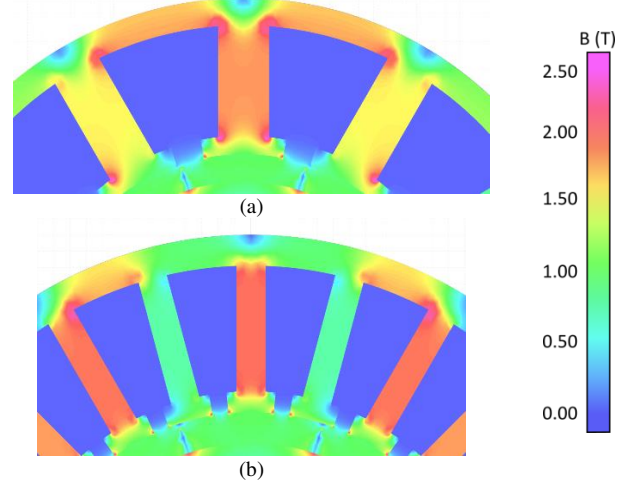

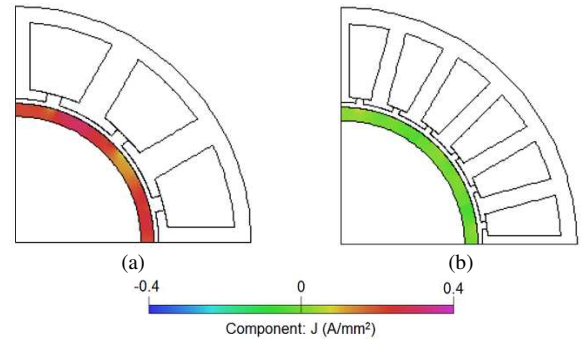Fig. 8. Flux density distribution of (a) 12s/10p, and (b) 24s/10p machines.

Fig. 9. Comparison of eddy current distribution in PMs. (a) 12s/10p, and (b) 24s/10p.

V. DUAL 3-PHASE MACHINE COMPARISON

It has been demonstrated thus far that the introduction of a second converter improves the electromagnetic performance of the stator-shifted machine with respect to the original single 3-phase machine. However, this comes at an increased cost for the overall system. If choosing a dual 3-phase design, then there are alternative similar slot-pole number combinations with double-layer windings that also offer harmonic elimination. This includes the 12s/10p dual 3-phase machine with 30° converter phase shift that eliminates the first subspace harmonic [14] and a 24s/10p stator shifted dual 3-phase machine that also eliminates the first harmonic while reducing the 7th [18]. These machines have been optimized using the same parameters as TABLE VIII and the onload torque results for the three dual 3-phase machines are comparatively plotted in Fig. 10, with results presented in TABLE XII. The single-layer machine offers the highest average torque performance at rated current of all machines and has a reduced torque ripple when compared with the 12s/10p double-layer machine. The losses of the dual 3-phase machines have also been calculated and are presented in TABLE XIII.
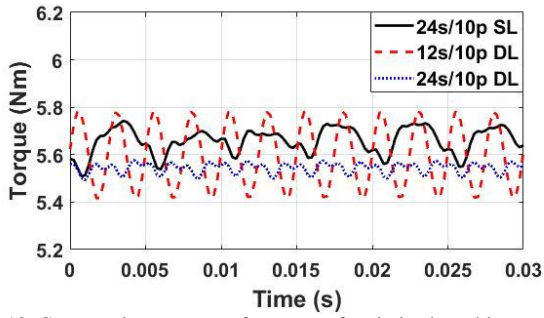
Fig. 10. Comparative torque performance of optimized machines.

TABLE XII TORQUE COMPARISON OF DUAL 3-PHASE MACHINES

	Average Torque (Nm)	Torque Ripple (%)
SL 24s/10p	5.66	0.233 (4.12%)
DL 12s/10p	5.60	0.369 (6.59%)
DL 24s/10p	5.54	0.085 (1.52%)

TABLE XIII LOSSES (IN W) AT RATED OPERATING CONDITIONS FOR DUAL 3-PHASE MACHINES

	Stator Loss	Rotor Loss	PM Loss	Copper Loss	Efficiency (%)
SL 24s/10p	4.56	4.728	0.0329	44.33	77.37
DL 12s/10p	3.73	0.665	0.0727	45.08	78.88
DL 24s/10p	4.51	0.805	0.0157	44.74	78.44

Both the 24s/10p machines exhibit similar stator loss which can be attributed to the increased saturation of the smaller teeth. Unfortunately, the single-layer machine still suffers from comparatively large rotor losses caused by the presence of the large first subspace harmonic, leading to a slightly reduced efficiency compared with the double-layer machines. However, the PM eddy current loss for the single-layer machine has been substantially reduced such that it lies between the two PM loss values for the double-layer machines. The combination of stator shifting and introduction of a second converter has yielded a machine which maintains higher torque as well as similar PM eddy current loss to the two double-layer dual 3-phase machine topologies. Therefore, the proposed machine could be a strong design choice where a simple winding structure is desired while reducing the risk of thermal demagnetization.

VI. EXPERIMENTAL VALIDATION

To validate the results of this work, a prototype 24s/10p machine was manufactured based on the specifications outlined in TABLE IV. The machine can be seen in Fig. 11.
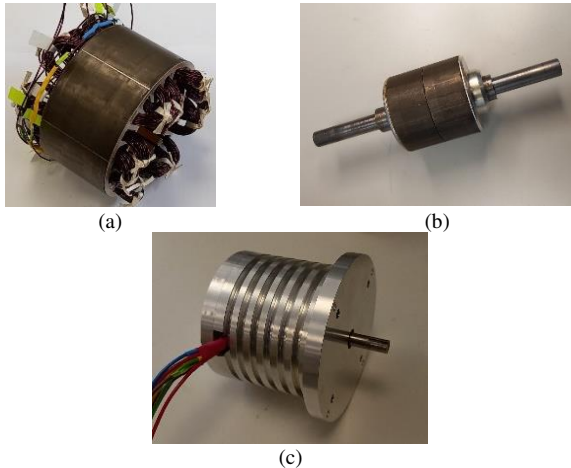

Fig. 11. Prototype machine. (a) 24-slot stator with 2 slot-pitch windings, (b) 10-pole rotor, and (c) entire machine with housing.
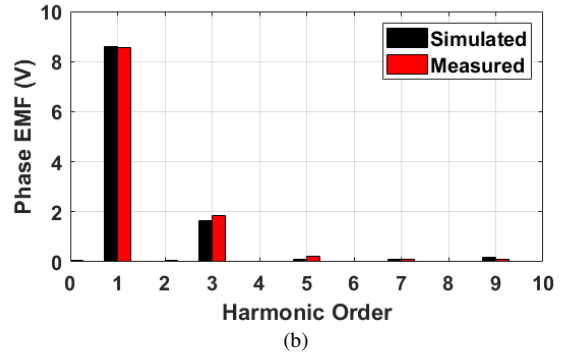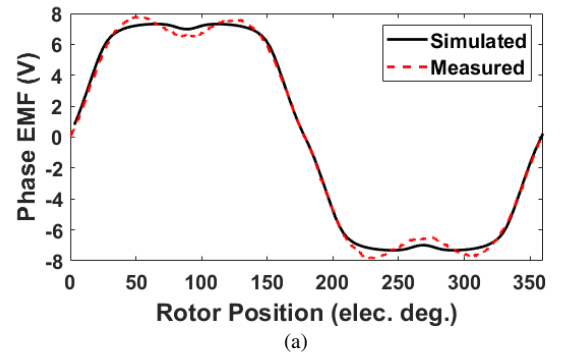

Fig. 12. Simulated and measured EMFs. (a) Waveforms, and (b) spectra.

A. EMF Measurements

The machine was spun at rated speed (400 RPM) and the EMF of a single phase was measured. Other phases will have the same EMF waveform but with a phase shift of 120 elec. deg. The measured EMF has been compared to the EMF obtained from simulations and is shown in Fig. 12. A strong agreement can be seen between the measured and simulated EMFs with both waveforms containing a 3rd order harmonic. There is a 0.45% reduction in the amplitude of the measured fundamental compared with the simulated result which is very small and could be attributed to manufacturing tolerance not accounted for in FEA, such as the stacking factor.

B. Static Torque Measurements

To validate the expected torque performance of the machine, torque measurements were carried out following the method outlined in [23]. This method can be used to measure both cogging torque and onload torque. However, for this prototype machine it was not possible to obtain the measured cogging torque. This is due to the periodicity of the cogging torque waveform being just 3 mech. deg. and the expected amplitude being 0.01Nm. The combination of error margin in measuring rotor position accurately to half a degree, coupled with 'noise' present in the system that could vary the torque even just a little made obtaining accurate results impossible. However, for static torque measurements the periodicity and amplitude are much larger allowing for accurate measurements. The experimental setup for these measurements can be seen in Fig. 13 (a).

Using two DC power supplies to excite the two winding sets such that $IA1 = IA2 = I$, $IB1 = IB2 = -I/2$ and $IC1 = IC2 = -I/2$, where I is the DC current, the static torque waveform of the machine could be measured through 360 elec. deg., as shown in Fig. 13 (b). The peak static torque at 90 elec. deg. phase angle was also measured at increasing phase currents and compared with the simulated results as shown in Fig. 13

(c). Similar as the EMFs, both measured torque results match well with their simulated counterparts.

C. Efficiency Measurements

To verify the simulated efficiency of the proposed winding structure, the machine was operated at a range of torque and speeds. For this, two 3-phase loads were connected to the prototype through a power analyzer with power into the system provided by a DC motor. The input power was measured using a torque transducer, and the phase resistances of the prototype were measured for accurate calculation of copper losses for the simulated machine comparison. The experimental setup and resulting efficiency plot for 400rpm and 800rpm can be seen in Fig. 14. The efficiency results show excellent agreement with simulated results, with only an average reduction in efficiency of 0.7% and 1.2% for 400rpm and 800rpm, respectively. In all cases, the power factor was between 0.997 and 1.0 as this is an SPM machine. As the proposed efficiency improvement of this machine was 3% when compared with a 12s/10p machine, the reduction of 0.7% and 1.2% is still well within a range that verifies the improved efficiency of the stator shifted dual 3-phase design.

VII. CONCLUSION

In this paper a method has been proposed for complete elimination of an unwanted higher order harmonic and reduction of the 1st order subharmonic in *m*-phase single-layer machines. This is achieved by doubling the number of slots then using the technique of stator shifting and operating the second *m*-phase winding set at a phase shift equivalent to $2\pi/N_s$. This methodology has been validated through both analytical modelling for 3- and 5-phase machines followed by FEA models of 24s/10p and 24s/14p dual 3-phase machines.

To investigate the impact of selected harmonic elimination on machine performance, FEA simulations were carried out showing that the 24s/10p machine can achieve higher average torque, reduced torque ripple, and an increased efficiency over the original 12s/10p machine. The 24s/14p machine is not as promising as it reduces the achievable torque slightly. However, the 24s/14p machine still reduces torque ripple and improves efficiency over the original 12s/14p machine thanks to its reduction in unwanted MMF harmonics. The 24s/10p dual 3-phase machine has been compared with two double-layer dual 3-phase machines and achieves the highest onload torque with similar PM eddy current losses. The primary benefit of this technique is the substantial reduction of PM eddy current losses that can lead to demagnetization of the PMs through heating.

ACKNOWLEDGMENT

For the purpose of open access, the author has applied a Creative Commons Attribution (CC BY) licence to any Author Accepted Manuscript version arising.

REFERENCES

[1] D. Ishak, Z. Q. Zhu, and D. Howe, "Analytical prediction of rotor eddy current losses in permanent magnet brushless machines with all teeth and alternate teeth windings—part i: Polar co-ordinate model," ICEMS, Lodz, Poland, Sept., 2004.
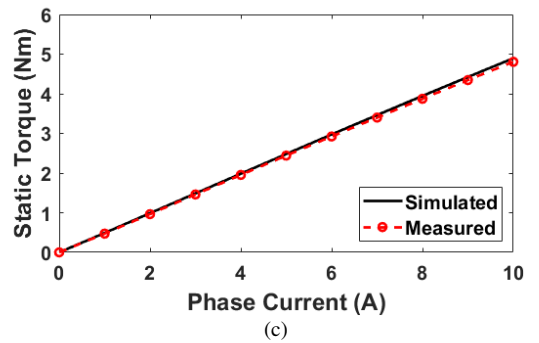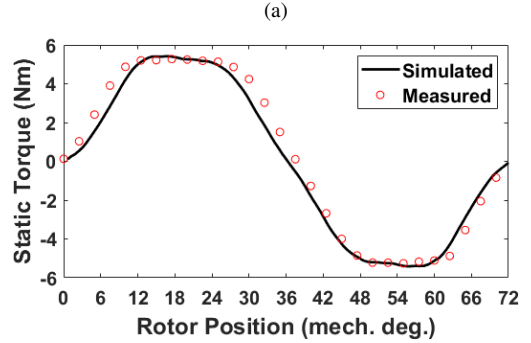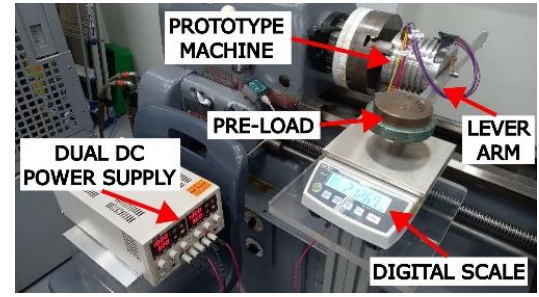

(a)

(b)

(c)

Fig. 13. Comparison between measured and simulated static torques. (a) Experimental setup, (b) static torque *vs* current phase angle and (c) peak static torque (at 90 elec. deg.) *vs* increasing phase current.
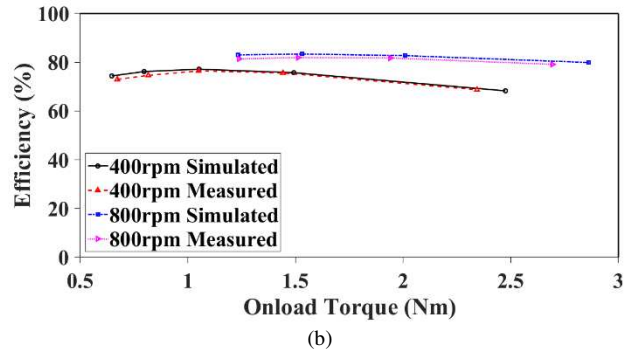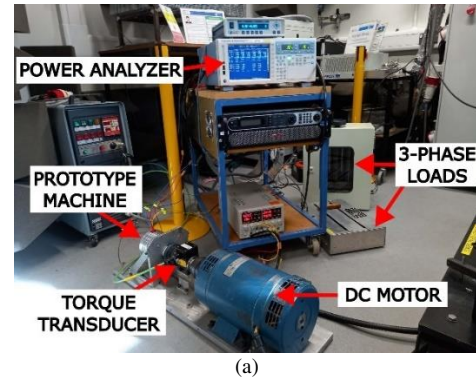

(a)

(b)

Fig. 14. Efficiency measurement. (a) Experimental setup, and (b) compared simulated and measured results.

[2] Z. Q. Z. D. Ishak, and D. Howe, "Analytical prediction of rotor eddy current losses in permanent magnet brushless machines with all teeth and alternate teeth windings—part ii: Rectangular co-ordinate model," ICEMS, Lodz, Poland, Sept., 2004.

[3] D. Ishak, Z. Q. Zhu, and D. Howe, "Comparative study of permanent magnet brushless motors with all teeth and alternative teeth windings," Second IEE International Conference on Power Electronics, Machines and Drives, Edinburgh, UK, Mar., 2004.

[4] A. M. El-Refaie, "Fractional-slot concentrated-windings synchronous permanent magnet machines: Opportunities and challenges," *IEEE Trans. Ind. Electron.,* vol. 57, no. 1, pp. 107-121, Jan. 2010.

[5] A. M. El-Refaie, T. M. Jahns, and D. W. Novotny, "Analysis of surface permanent magnet machines with fractional-slot concentrated windings," *IEEE Trans. Energy Convers.,* vol. 21, no. 1, pp. 34-43, Mar. 2006.

[6] Z. Q. Zhu and D. Howe, "Influence of design parameters on cogging torque in permanent magnet machines," in *IEEE International Electric Machines and Drives Conference Record*, Milwaukee, WI, USA, May 1997.

[7] N. Bianchi, S. Bolognani, M. D. Pre, and G. Grezzani, "Design considerations for fractional-slot winding configurations of synchronous machines," *IEEE Trans. Ind. Appl.,* vol. 42, no. 4, pp. 997-1006, July 2006.

[8] A. M. El-Refaie, Z. Q. Zhu, T. M. Jahns, and D. Howe, "Winding inductances of fractional slot surface-mounted permanent magnet brushless machines," in *2008 IEEE Industry Applications Society Annual Meeting*, Edmonton, Alberta, Canada, Oct. 2008.

[9] N. Bianchi and M. D. Pre, *Use of the star of slots in designing fractional-slot single-layer synchronous motors* (Proc. Inst. Elect. Eng.—electr. Power appl). 2006.

[10] G. Dajaku and D. Gerling, "A novel 24-slots/10-poles winding topology for electric machines," in *2011 IEEE International Electric Machines & Drives Conference (IEMDC)*, Ontario, Canada, May 2011.

[11] P. B. Reddy, K.-K. Huh, and A. M. El-Refaie, "Generalized approach of stator shifting in interior permanent-magnet machines equipped with fractional-slot concentrated windings," *IEEE Trans. Ind. Electron.,* vol. 61, no. 9, pp. 5035-5046, Sept. 2014.

[12] K. Wang, Z. Q. Zhu, and G. Ombach, "Synthesis of high performance fractional-slot permanent-magnet machines with coil-pitch of two slot-pitches," *IEEE Trans. Energy Convers.,* vol. 29, no. 3, pp. 758-770, 2014-09-01 2014, doi: 10.1109/tec.2014.2318173.

[13] H. Y. Sun and K. Wang, "Space harmonics elimination for fractional-slot windings with two-slot coil pitch," *IEEE Access,* vol. 7, pp. 106961-106972, 2019-01-01 2019, doi: 10.1109/access.2019.2933256.

[14] Z. Zhu, S. Wang, B. Shao, L. Yan, P. Xu, and Y. Ren, "Advances in dual-three-phase permanent magnet synchronous machines and control techniques," *Energies,* vol. 14, no. 22, p. 7508, Nov. 2021.

[15] P. Xu *et al.*, "Analysis of dual three-phase permanent-magnet synchronous machines with different angle displacements," *IEEE Trans. Ind. Electron.,* vol. 65, no. 3, pp. 1941-1954, Mar. 2018.

[16] A. M. El-Refaie, M. R. Shah, R. Qu, and J. M. Kern, "Effect of number of phases on losses in conducting sleeves of surface pm machine rotors equipped with fractional-slot concentrated windings," *IEEE Trans. Ind. Appl.,* vol. 44, no. 5, pp. 1522-1532, Sept. 2008.

[17] X. Chen, J. Wang, V. I. Patel, and P. Lazari, "A nine-phase 18-slot 14-pole interior permanent magnet machine with low space harmonics for electric vehicle applications," *IEEE Trans. Energy Convers.,* vol. 31, no. 3, pp. 860-871, Sept. 2016.

[18] A. S. Abdel-Khalik, S. Ahmed, and A. M. Massoud, "A six-phase 24-slot/10-pole permanent-magnet machine with low space harmonics for electric vehicle applications," *IEEE Trans. Magn.,* vol. 52, no. 6, pp. 1-10, June 2016.

[19] B. Zhao *et al.*, "A novel five-phase fractional slot concentrated winding with low space harmonic contents," *IEEE Trans. Magn.,* vol. 57, no. 6, pp. 1-5, 2021-06-01 2021, doi: 10.1109/tmag.2021.3057650.

[20] S. Xie *et al.*, "Harmonic reduction for two-slot pitch winding permanent magnet vernier machines with stator shifting technique," in *IECON 2021 – 47th Annual Conference of the IEEE Industrial Electronics Society*, Toronto, Canada, Oct. 2021.

[21] I. Rudden, G.-J. Li, Z.-Q. Zhu, A. Duke, Z. Azar, and A. Thomas, "Stator shifting in dual m-phase spm machines with single-layer windings for space harmonic cancellation," in *2023 26th International Conference on Electrical Machines and Systems (ICEMS)*, 2023-11-05 2023: IEEE, doi: 10.1109/icems59686.2023.10345143.

[22] J. Feng *et al.*, "Comparative study of dual 3‐phase permanent magnet machines with coil span of two slot‐pitches," *IET Electric Power Applications,* vol. 16, no. 12, pp. 1426-1438, Dec. 2022.

[23] Z. Q. Zhu, "A simple method for measuring cogging torque in permanent magnet machines," in *IEEE Power & Energy Society General Meeting*, July 2009: IEEE.